

# Sicherstellung der Dauerhaftigkeit von Stahlbetonbauten bei Karbonatisierung

ETH Zürich, Institute for Building Materials

Dr. Matteo Stefanoni  
Prof. Dr. Bernhard Elsener  
Prof. Dr. Ueli Angst

cemsuisse-Projekt 201807 – Dezember 2020

Diese Forschungsarbeit wurde durch cemsuisse, Verband der Schweizerischen Cementindustrie mitfinanziert.

## **Vorwort der Begleitgruppe**

Cemsuisse hat in der Vergangenheit eine Reihe von Untersuchungen zur Dauerhaftigkeit von Stahlbetonbauwerken, insbesondere zur Karbonatisierung von Beton von mehreren Forschungsstellen durchführen lassen. In dem vorliegenden Forschungsbericht der Forschergruppe von Prof. U. Angst von der ETH Zürich wurde die Karbonatisierung des Betons im Hinblick auf die Korrosion einer Stahlbewehrung systematisch untersucht. Dabei wurde eine umfangreiche Studie mit materialtechnologischen und umwelttechnischen Parametern vorgenommen.

Es hat sich gezeigt, dass der Feuchtigkeitsgehalt des Betons die wesentliche Einflussgrösse für die Korrosion einer Stahlbewehrung in karbonatisiertem Beton ist. Korrosion der Stahlbewehrung in karbonatisiertem Beton tritt nur ein, wenn eine relative Luftfeuchtigkeit von grösser als 99 % im Beton vorliegt.

Mit diesem Ergebnis konnten die normativen Anforderungen an den Karbonatisierungswiderstand für die Expositionsklasse XC3 gemäss SN EN 206 angepasst werden kann, indem eine Erhöhung des Grenzwertes des Karbonatisierungswiderstandes sowohl beim Mittelwert als auch beim Mittelwert plus Grenzwertabweichung durchgeführt wurde. Mit dieser Korrektur wird das Karbonatisierungs- und Korrosionsverhalten bei der Expositionsklasse XC3 nicht mehr überschätzt und realitätsnäher betrachtet, wodurch unnötig hohe Anforderungen für die Praxis vermieden werden können.

*Dr. Peter Lunk, Leiter Technical Expert Center, Holcim (Schweiz) AG*

*Dr. P. Kruspan, Produktmanager, Holcim (Schweiz) AG*

## **cemsuisse Forschungsförderung**

Die cemsuisse Forschungsförderung unterstützt Forschungsprojekte im Bereich der Betonanwendung, welche von kompetenten Forschergruppen an cemsuisse herangetragen werden. Mit der proaktiven Forschungsförderung definiert cemsuisse zudem Forschungsprojekte von spezifischem Interesse und trägt diese an kompetente Forschergruppen heran oder schreibt sie öffentlich aus. Die Projektnehmer werden jeweils von einer Begleitgruppe aus cemsuisse-Vertretern fachlich unterstützt.

*Dr. Martin Tschan, Leiter Umwelt, Technik, Wissenschaft, cemsuisse*

## Table of Contents

1.	Abstract .....	3
2.	Introduction .....	4
3.	Research objective .....	5
4.	Experimental.....	6
4.1.	Phase 1 .....	6
4.2.	Phase 2 .....	8
5.	Results.....	11
5.1.	Phase 1 .....	11
5.2.	Phase 2 .....	15
6.	Discussion .....	20
6.1.	Comparison between corrosion rates of Phase 1 and Phase 2 .....	20
6.2.	Relationship between corrosion rate and capillary porosity in Phase 2 .....	21
6.3.	Influence of the aggregates on carbonation-induced corrosion rate .....	21
6.4.	Factors influencing the corrosion rate .....	22
7.	Conclusions .....	23
8.	Outlook .....	24
8.1.	On the important role of moisture in the concrete cover .....	24
8.2.	Amount of corrosion leading to damage (cracking, spalling).....	24
9.	References .....	25

# 1. Abstract

This report describes the work of CEMSUISSE research project „Sicherstellung der Dauerhaftigkeit von Stahlbetonbauten bei Karbonatisierung“. The corrosion rate of steel in carbonated cementitious materials was studied in both small fine mortar samples with embedded carbon steel wires, and in concrete with embedded carbon steel rebars. Both experimental setups allowed for the monitoring of the instantaneous corrosion rate through non-destructive electrochemical techniques. The advantage of the small samples is that they allowed for a fast carbonation and equilibration to environmental changes (e.g. humidity, temperature) and thus a fast screening of a large set of variables. The larger concrete samples were used to confirm the results from the fine mortar samples for selected cases. Four different binders were studied in the experimentation (CEM I 42.5 N, CEM II/B-LL 32.5 R, CEM II B/-M (T-LL) 42.5 N, CEM III/B 42.5 L), and the water to binder (w/b) ratio was varied (0.5 and 0.6). Additionally, the influence of aggregate size distribution was investigated in small scale experiments. Regarding environmental variables, the corrosion rate was studied for a range of high humidity conditions (95% RH, 99% RH and WET, that is, in contact with liquid water), as it is well known that the corrosion rate in carbonated concrete in dry environment is not of concern. Also, the influence of temperature was considered and corrosion rates were measured in a range of temperatures between 5 and 40 °C. The results show that the humidity of the environment is the parameter that has the highest impact on the measured corrosion rate, with an increase of a factor 10 when going from 95% RH to WET exposure. The temperature, in the studied range, had a moderate impact, with a change of a factor 3 between 5 and 40 °C. The mix design parameters had the weakest impact on the corrosion rate. The aggregate size did not show any influence, the w/b affected the corrosion rate only by a factor <2 and the binder type showed an effect up to a factor 3. The corrosion rate values measured on the small-scale mortar samples were similar to those measured on the concrete samples. Thus, the applicability of the measurements performed on the small samples for more realistic conditions could be confirmed.



## 2. Introduction

One of the main degradation processes of reinforced concrete structures comes from its carbonation [1, 2]. Carbonation means the progressive neutralization of the alkaline constituents of concrete by  $\text{CO}_2$  in the air forming mainly calcium carbonate. When carbon dioxide enters the pore structure, it dissolves in the pore solution and neutralizes the initially high alkalinity ( $\text{pH} > 13$ ), this high pH is the reason why steel in concrete is protected from corrosion. Consequently, the reinforcing steel is depassivated and can corrode, leading to damage of the concrete. Indeed, corrosion of steel in carbonated concrete was a major concern of research and practice in the years from 1950 to 1990. The research findings led to the requirement of dense concrete (lower w/b ratio), the control of concrete properties and to a marked increase in the cover depth (from 20 mm to 35 mm) in the codes of practice. The European standard on concrete EN 206-1 [3] published in the year 2000 classified the risk of carbonation-induced corrosion depending on the severity of the environment (XC1 to XC4). With the minimum requirements given in the recommendations (maximum w/b ratio, minimum cement content, minimum cover depth), the codes of practice since then give guidance for reinforced concrete made with Portland cement (CEM I) on how to avoid carbonation induced corrosion for structures with expected service life of 50 or 100 years.

The Swiss standard SIA 262, in appendix I, specifies a test called “carbonation resistance” and stipulates thresholds for the resulting parameter  $k_N$ , which essentially is a carbonation coefficient in the commonly used square-root-of-time approach to predict carbonation ingress into concrete. With this approach, it shall be ensure that during the entire service life the (average) carbonation depth does not (XC4) or very late (XC3) reach the reinforcing steel. The corrosion propagation stage, the stage during which corrosion occurs and leads to damage, however, is not explicitly considered.

The role of carbonation as a factor that contributes to the degradation of reinforced concrete is becoming increasingly important again for two reasons: first, many old reinforced concrete structures that were built before modern standards were applied are ageing and have to be maintained. Secondly, the need to reduce  $\text{CO}_2$  emissions and to obtain materials having a reduced environmental footprint is leading to a reduction of the clinker content in the cements [4, 5]. The new environmentally friendly binders are more susceptible to carbonation than Portland cement, as their alkalinity reserve ( $\text{Ca}(\text{OH})_2$ ) is more limited [6].

In order to reliably predict the service life of concrete structures in carbonation exposure, it is necessary to implement the corrosion propagation stage. For this to be possible, one needs to know how fast the embedded steel is going to corrode in a defined environment. Recent advances in the understanding of the corrosion process in carbonated concrete suggest that the key parameters that control the rate of corrosion are the pore structure of the carbonated cementitious material and the water content inside the pores [7, 8]. However, in practice, several factors can affect the corrosion propagation rate. Some of these are temperature and humidity at the rebars depth. The combination of these two is critical, as it is known that corrosion is very much affected by these parameters [7, 8, 9, 10, 11]. In this project we tried to isolate some of these variables, in order to quantify the influence of each variable (both environmental and material) independently of the others. As a result, it is shown what parameters have the most important effect and in which conditions corrosion rates induced by carbonation might reach values of concern.

### 3. Research objective

The objective of this project is to study the corrosion rate of steel embedded in carbonated cementitious materials, with particular focus on i) selected binder types, ii) differences between mortar and concrete, iii) influences related to the environmental exposure conditions, namely moisture and temperature. By defining in which conditions the carbonation-induced corrosion of steel can reach rates of concern, we seek to facilitate the implementation of the corrosion propagation stage in approaches towards ensuring durability and sustainability of reinforced concrete structures in carbonation exposure environments.

## 4. Experimental

The experimentation was divided in two main phases:

Phase 1: Initial screening of influencing parameters by means of small mortar samples with thin steel wires embedded, such as humidity and temperature of exposure, aggregate size and binder type.

Phase 2: Confirmation of results from the first experimentation by means of actual concrete samples with real rebars embedded. In this second part, a lower number of samples and variables would be studied due to the lengthy nature of the experiments for large samples.

### 4.1. Phase 1

#### 4.1.1. Sample design

The test setup consists of small mortar samples ( $8 \times 8 \times 0.6 \text{ cm}^3$ ). They are instrumented with 5 carbon steel wire electrodes (cover depth from both sides 3 mm), a reference electrode (Ag/AgCl), and a stainless-steel grid counter electrode (Figure 1). The thin sample design allows for rapid full carbonation (max 3 weeks in 4%  $\text{CO}_2$ ) and for equilibration with environmental humidity in a short time [12, 13].

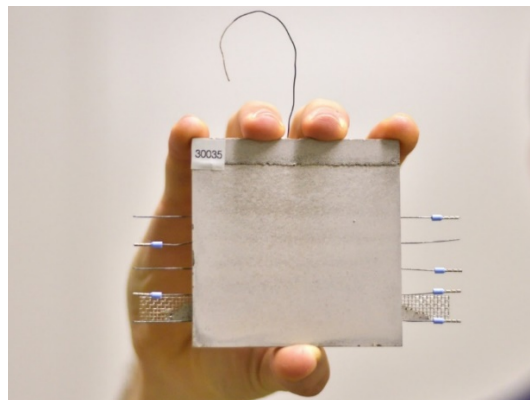


Figure 1. Small mortar specimens used for the screening of phase 1.

#### 4.1.2. Materials

Four different cement types commonly used in Switzerland were investigated: CEM I 42.5 N, CEM II/B-M (T-LL) 42.5 N, CEM II/B-LL 32.5 R, CEM III B 42.5 L. For reasons of readability, these will in this report be referred to as CEM I, CEM II/B-M, CEM II/B-LL, and CEM III/B, respectively.

The w/b ratios tested were 0.5 and 0.6; the sand/binder ratio was 2 by weight and the sand had a maximum particle diameter ( $\phi_s$ ) of 1 mm. The specimens were demoulded after one day and cured at 95% RH for 7 days before being carbonated.

#### 4.1.3. Carbonation procedure

The samples were carbonated in a carbonation chamber at 20°C, 57% relative humidity and 4% CO<sub>2</sub> concentration. CEM II and CEM III mortars were carbonated for 2 weeks and CEM I mortars for 3 weeks, until complete carbonation.

#### 4.1.4. Aggregate size

In order to test the possible influence on the corrosion rate of the aggregate size distribution and extent of interfacial transition zone (ITZ), the aggregate content was varied. For this, CEM II/B-M (T-LL) was used with a w/b of 0.5. The sand component of the mortar was sieved in different fractions (S1,  $\phi_s < 0.25\text{mm}$ ; S2,  $0.25 < \phi_s < 0.5\text{mm}$ ; S3,  $0.5 < \phi_s < 1\text{mm}$ ). Each fraction was used for different samples without changing the total mass of aggregate in the mix.

#### 4.1.5. Exposure conditions

**Constant relative humidity:** After carbonation, the samples were studied in different exposure conditions of controlled and constant environments: 95% RH and 99% RH; at a constant temperature of 20 °C. The relative humidity was controlled by means either of climatic conditioning rooms (95% RH) or ultrapure water (99% RH), taking care no water condensation would take place in the container by keeping the temperature constant.

**Wet and dry cycles:** For cyclic exposure (Figure 2), the samples were exposed to demineralized water (pond mounted with a silicon sealed wall). For wetting, 3 mm of demineralized water was placed on the samples; for drying, the samples were exposed to laboratory climate (approx. 30-40% RH). Up to 6 cycles were carried out.

**Temperature:** The influence of temperature was tested by performing the wetting cycles in controlled temperature environments (laboratory ambient temperature, 21 °C; climatic chambers, 5, 10, 30 and 40 °C). For this, only the wet exposure was tested, in order to decouple the temperature influence from the moisture content, which is different at different temperatures for the same relative humidity.

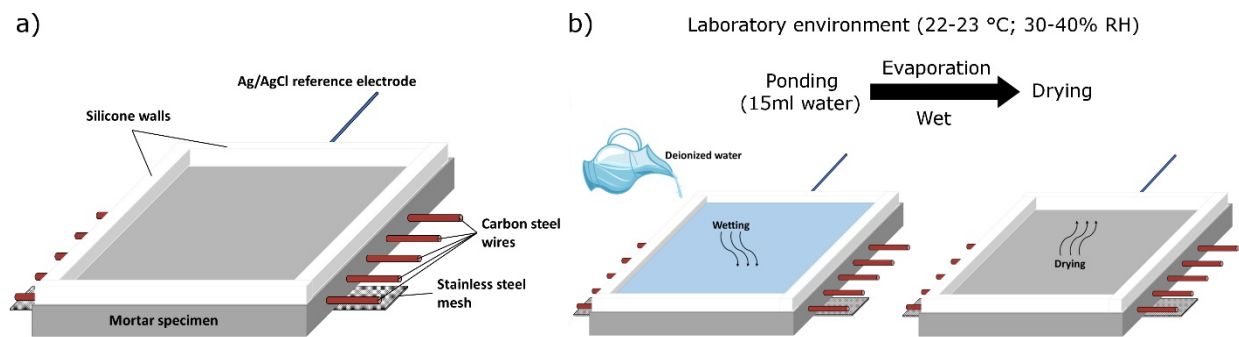


Figure 2. a) schematic illustration of the mortar specimen's configuration (8x8x0.6 cm³). b) Representation of the procedure used for ponding and drying of the samples.

## 4.2. Phase 2

### 4.2.1. Sample design

The test setup consists of concrete samples (15x15x4 cm<sup>3</sup>). They were instrumented with 3 carbon steel rebars (diameter = 6 mm, cover depth from both sides = 15 mm), a reference electrode (Ag/AgCl), and a stainless steel grid counter electrode (Figure 3a).

### 4.2.2. Materials

The same binders as in Phase 1 were investigated: CEM I 42.5 N, CEM II/B-M (T-LL) 42.5 N, CEM II/B-LL 32.5 R, CEM III B 42.5 L. The w/b ratios tested were 0.5 and 0.6; the aggregate/binder ratio was 3 by weight and the maximum aggregate size was ( $\phi_s$ ) 8 mm. The specimens were demoulded after one day and cured at 95% RH for 3 months before being carbonated.

### 4.2.3. Carbonation procedure

The samples were carbonated in a carbonation chamber that was designed and built in house. The environmental conditions inside the box were: 21-23 °C, 65-75% RH and 50-100% CO<sub>2</sub> concentration. Companion samples (approx. 4x4x4 cm<sup>3</sup>) were periodically cut and analysed by phenolphthalein test, in order to check the carbonation level. Once the companion samples showed complete carbonation, depending on the binder type and w/b, the respective specimens were extracted from the chamber for starting the corrosion rate testing.

*Carbonation chamber:* the in-house carbonation chamber consists of a sealed glovebox (Figure 3b), provided with a gas inlet and outlet for flushing with CO<sub>2</sub>. The parameters inside the glovebox (Temperature, Pressure, CO<sub>2</sub> content and Relative Humidity) were monitored online by means of an ExplorIR®-M 100% CO<sub>2</sub> Sensor, purchased from CO<sub>2</sub> Meter.

### 4.2.4. Natural carbonation

One set of companion specimens was stored in a climatic room at 20°C and 65% RH. These specimens were exposed to what is here considered “natural carbonation” (not accelerated by means of increased CO<sub>2</sub> concentration) and were tested periodically over time. As natural carbonation requires a very long time to happen, the testing of these specimens will continue after the end of the project that is the subject of this report.

### 4.2.5. Exposure condition

*Constant relative humidity:* After carbonation, the samples were studied at 95% RH at a constant temperature of 20 °C. The relative humidity was controlled by means a climatic conditioning room (95% RH).

*Wet and dry cycles:* For cyclic exposure, the samples were exposed to demineralized water (pond mounted with a silicon sealed wall). For wetting, demineralized water was placed on the samples; the wetting was prolonged up to 7 days, until stable values over time could be measured. For drying, the samples were exposed to laboratory climate (approx. 30-40% RH). Up to 6 cycles were carried out.



#### 4.2.6. Porosity

In order to characterize the concrete porosity that could be filled by water, once carbonation was complete, the companion specimens used to check the carbonation progress were cut in slices (approx. 0.5-1 cm thick). The slices were dried following the procedure: 1 week immersion in isopropanol for solvent exchange procedure (most of the water is replaced by isopropanol); following to that, the slices were dried in an oven at 60 °C until constant weight. When constant weight was achieved, the slices were immersed in ultrapure water and the weight gain was recorded. The volume of the slices was calculated by measuring all the sides with a caliper. The mass difference was converted into porosity with the following equations:

$$V_w = (W_{wet} - W_{dry}) / \rho_w \quad (1)$$

$$P = V_w / V_c \quad (2)$$

Where  $V_w$  is the water volume that was absorbed by the concrete,  $W$  is the weight of the concrete slices,  $\rho_w$  is the density of water (assumed as 1 kg/l),  $P$  is the porosity and  $V_c$  is the volume of the concrete slice.



Figure 3 a) Concrete specimens for corrosion rate measurements in Phase 2. b) Carbonation box.

#### 4.2.7. Corrosion rate measurements

All the electrochemical experiments were performed using a potentiostat Metrohm Autolab PGSTAT30. As a reference electrode, the embedded Ag/AgCl sensor was used, its reference potential was periodically calibrated against an external Ag/AgCl reference electrode. The embedded carbon steel (wires or rebars) was used as working electrode, while the stainless-steel grid was used as counter electrode. The instantaneous corrosion current density was determined by linear polarization resistance (LPR) measurements [14]. The LPR was measured at  $\pm 10$  mV around the open circuit potential with a scan rate of 0.1 mV/s. The mortar IR-drop was measured by impedance spectroscopy measurements (50 frequencies logarithmically distributed between  $10^5$  and 10 Hz). The impedance measurements were performed right after each polarization resistance test. The ohmic resistance ( $R_\Omega$ ) was extrapolated by fitting the first semicircle appearing in the Nyquist

plot and considering the value first intercepted on the real impedance axis. The obtained  $R_{\Omega}$  was subtracted from the total resistance  $R_p'$  to get the IR-free polarization resistance values  $R_p$ .

The Stern Geary relation was used to calculate the corrosion rate (eq. 3):

$$i_{corr} = B/R_p \quad (3)$$

Where  $B$  is a parameter depending on the electrochemical properties of the considered system; commonly a value of 26 mV is used for iron in actively corroding state [15]. In order to calculate the corrosion current density, the steel embedded surface area was considered (approx. 30 cm<sup>2</sup>).

## 5. Results

### 5.1. Phase 1

Table 1 summarizes the corrosion rate measurements of phase 1, performed on the small mortar samples. The data in the table is the result of monitoring the corrosion rate over time, the results reported include an average and standard deviation of at least 4 measurements per sample type and exposure condition. The values in the table are the corrosion rates at steady state, that is when the corrosion rate has stabilized and is constant.

*Table 1 Summary of all corrosion rates of Phase 1. What is reported is an average over at least 3 measurements per mix and exposure condition, with the relative standard deviation. Note that 1  $\mu\text{A}/\text{cm}^2$  corresponds to approx. 12  $\mu\text{m}/\text{y}$ .*

		Corrosion rate ( $\mu\text{A}/\text{cm}^2$ )							
Binder		CEM I 42.5 N		CEM II/B-LL 32.5 R		CEM II/B-M 42.5 N		CEM III/B 42.5 L	
w/b		0.5	0.6	0.5	0.6	0.5	0.6	0.5	0.6
Moisture state	95% RH	0.21 $\pm 0.07$	0.30 $\pm 0.03$	0.26 $\pm 0.03$	0.32 $\pm 0.01$	0.14 $\pm 0.03$	0.20 $\pm 0.02$	0.30 $\pm 0.03$	0.34 $\pm 0.05$
	99% RH	0.74 $\pm 0.24$	0.88 $\pm 0.30$	0.77 $\pm 0.05$	1.06 $\pm 0.26$	0.45 $\pm 0.10$	0.58 $\pm 0.06$	0.58 $\pm 0.09$	0.82 $\pm 0.11$
	WET	0.85 $\pm 0.21$	1.17 $\pm 0.52$	1.53 $\pm 0.54$	2.14 $\pm 0.46$	0.86 $\pm 0.15$	1.37 $\pm 0.30$	1.53 $\pm 0.93$	2.26 $\pm 0.86$
Temperature ( $^{\circ}\text{C}$ ) (WET)	5	0.33 $\pm 0.1$	0.53 $\pm 0.20$	0.61 $\pm 0.14$	1.33 $\pm 0.35$			0.92 $\pm 0.53$	1.25 $\pm 0.34$
	10			1.18 $\pm 0.34$	1.54 $\pm 0.33$			1.23 $\pm 0.57$	1.64 $\pm 0.63$
	21	0.85 $\pm 0.21$	1.17 $\pm 0.52$	1.53 $\pm 0.54$	2.14 $\pm 0.46$			1.53 $\pm 0.93$	2.26 $\pm 0.86$
	30	1.22 $\pm 0.02$	1.66 $\pm 0.22$	2.00 $\pm 0.63$	2.69 $\pm 0.52$			2.02 $\pm 0.90$	2.72 $\pm 1.10$
	40	1.21 $\pm 0.03$	1.96 $\pm 0.29$	2.19 $\pm 0.49$	2.80 $\pm 0.57$			2.54 $\pm 1.21$	3.02 $\pm 1.33$
Aggregate size distribution (95% RH)	S1					0.13 $\pm 0.01$			
	S2					0.18 $\pm 0.019$			
	S3					0.15 $\pm 0.013$			

### 5.1.1. Influence of the binder type and w/b

Figure 4a shows the corrosion rates for the different binder types and for the different moisture states. It appears that steel electrodes imbedded in CEM II/B-LL and CEM III/B corrode slightly faster than in CEM I and CEM II/B-M. However, the difference between binders remains always lower than a factor 2. Therefore, the binder type does not seem to impact the corrosion rate drastically. The same applies for the w/b, Figure 4b shows the data grouped to highlight only the w/b effect. This effect seems to be even lower than the one of the binder type, at least in the range that was studied in our work (w/b 0.5 and 0.6).

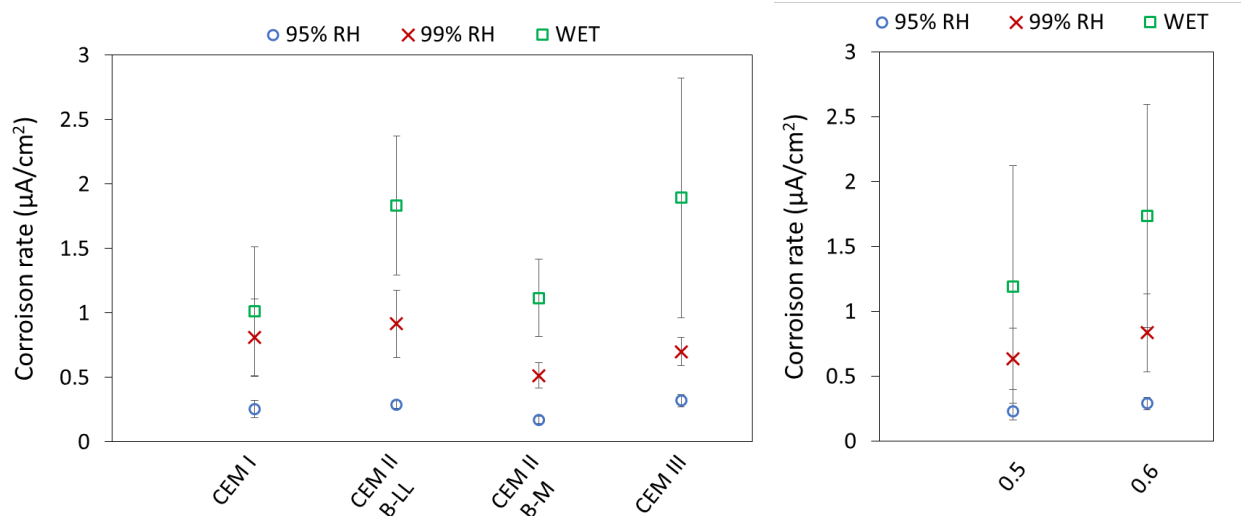


Figure 4 Corrosion rates grouped per binder type (a) and w/b (b). The markers are the average of all corrosion rates measured for a specific binder (a) or w/b (b), the whiskers are the standard deviation. Note that  $1 \mu\text{A}/\text{cm}^2$  corresponds to approx.  $12 \mu\text{m}/\text{y}$ .

### 5.1.2. Influence of humidity exposure condition

The humidity of exposure seems to be a far more important parameters compared to binder type and w/b ratio (Figure 5). Even in a range of humidity that may be perceived as somewhat restricted, passing from 95% RH to WET condition, an increase in corrosion rate of a factor 10 was observed.

Figure 5 depicts the limits that are usually considered for a rough estimation of the corrosion risk. Only in WET conditions is the corrosion rate just above the threshold of medium risk, while for 95% RH and 99% RH the values are in the low risk range.

### 5.1.3. Influence of temperature

The tests related to the influence of temperature gave very consistent results. For all the tested specimens, the corrosion rate increase as a function of temperature was constant (Figure 6). An increase of temperature of  $35^\circ\text{C}$  (from  $5^\circ\text{C}$  to  $40^\circ\text{C}$ ) led to a corrosion rate increase of a factor less than 3. The differences between different mixes was almost constant over the whole range of temperatures.

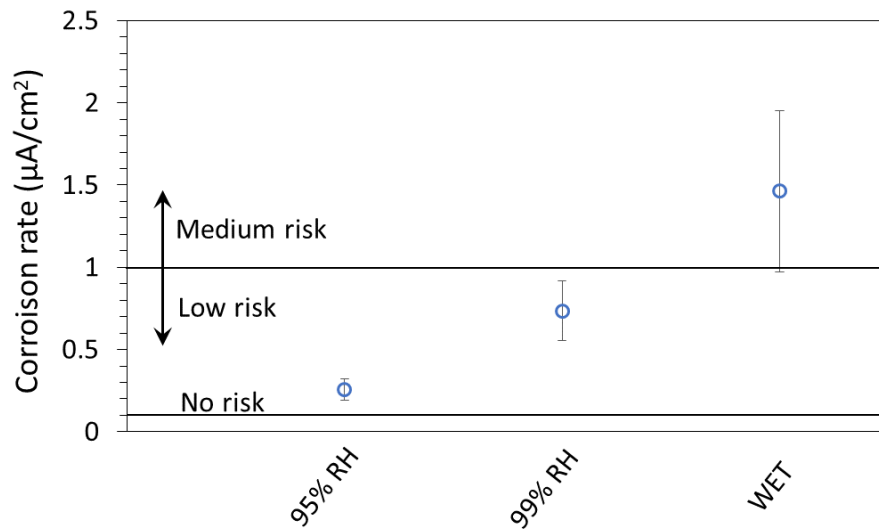


Figure 5 Corrosion rates grouped per humidity exposure condition. The markers are the average of all corrosion rates measured at the specific humidity condition; the whiskers are the standard deviation. Note that 1  $\mu\text{A}/\text{cm}^2$  corresponds to approx. 12  $\mu\text{m}/\text{y}$ . The thresholds (medium, low, no risk) are based on L. Bertolini et al. "Corrosion of Steel in Concrete", WILEY-VCH, 2003).

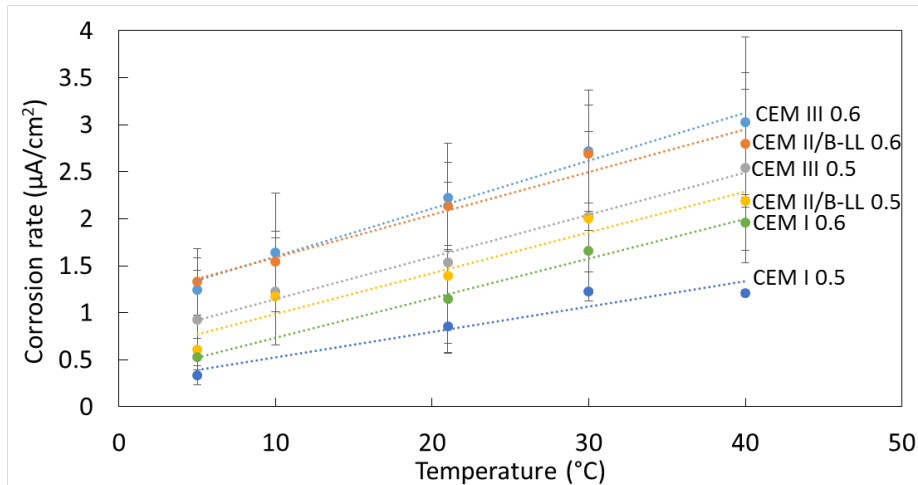


Figure 6 Corrosion rate of the different mixes at different temperatures. The markers are the average of at least 3 corrosion rate measurement per each mix and temperature, the whiskers are the standard deviation. Note that 1  $\mu\text{A}/\text{cm}^2$  corresponds to approx. 12  $\mu\text{m}/\text{y}$ .

#### 5.1.4. Influence of aggregate size distribution

Finally, the results of the tests carried out to investigate the influence of the aggregate size distribution turned out to be inconclusive. There was no trend or recognizable dependence of the corrosion rate on this parameter apparent. Figure 7 shows that the corrosion rate in the three different mixes that were tested did not depend on the size of the sand that was used.



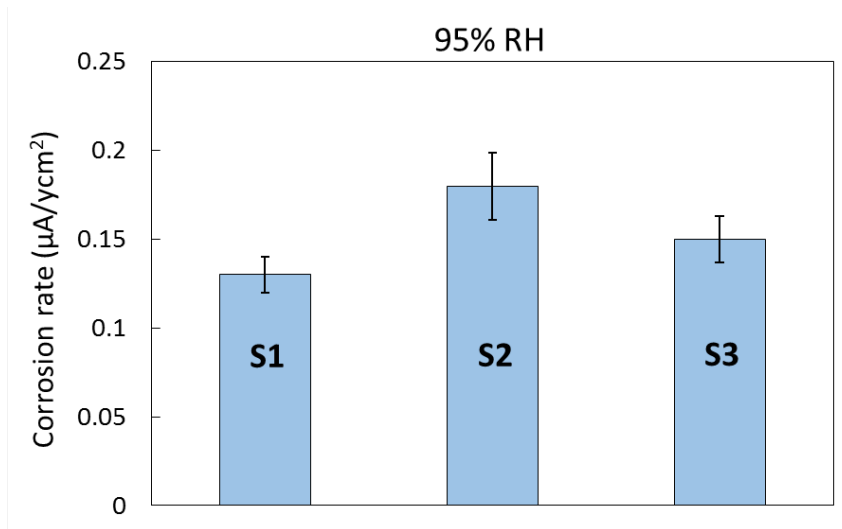


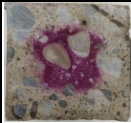


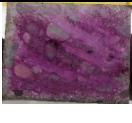

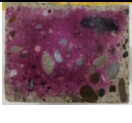


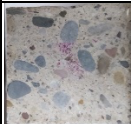
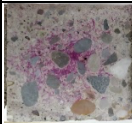

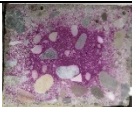

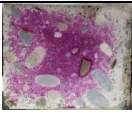


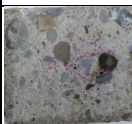

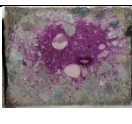
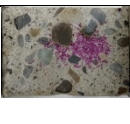
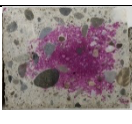
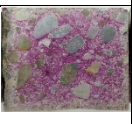
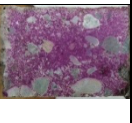
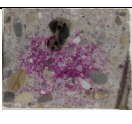
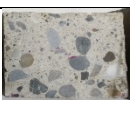
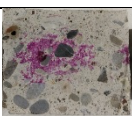





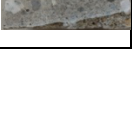
Figure 7 Corrosion rate of mortar samples produced with one binder and w/b (CEM II/B-M 0.5) and different aggregate sizes. From fine to coarse  $S1 < S2 < S3$ . Exposure at 95% RH. Note that  $1 \mu\text{A}/\text{cm}^2$  corresponds to approx.  $12 \mu\text{m}/\text{y}$ .

## 5.2. Phase 2

### 5.2.1. Concrete accelerated carbonation

From the periodic measurements of the carbonation penetration in the accelerated carbonation tests (Table 2), it seems the most susceptible binder is CEM II/B-LL. It took only 3 weeks to completely carbonate the specimen with w/b 0.6, while the 0.5 required approximately 5 weeks. CEM II/B-M and CEM III show an intermediate and similar carbonation rate, with a carbonation time of approx. 6-7 weeks for the w/b 0.6 and 10-11 weeks for w/b 0.5. As expected, CEM I is by far the most resistant, as it took 16 weeks for the w/b 0.6 and 22 weeks for the 0.5.

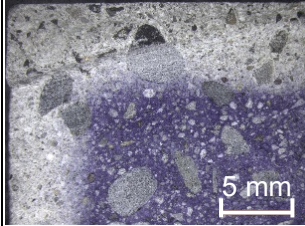
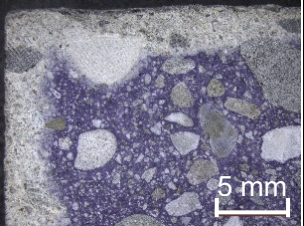
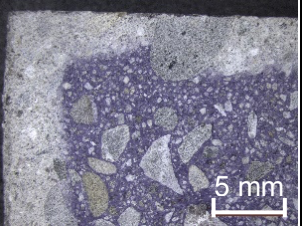
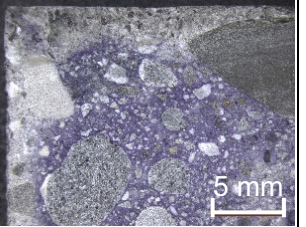
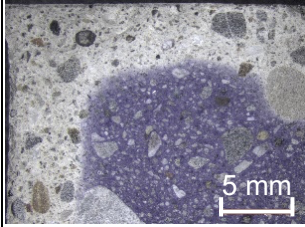
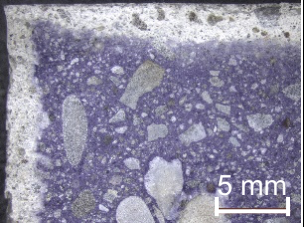
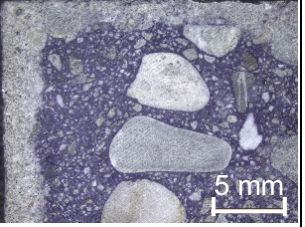
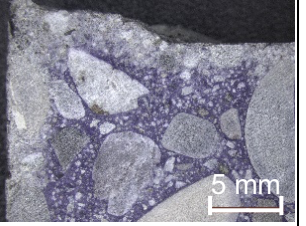
Table 2 Phenolphthalein test to assess the accelerated carbonation for the different concrete mixes. The slices in the pictures are approx. 4 cm x 4 cm.

Time	CEM II B-LL 0.6	CEM II B-LL 0.5	CEM II B-M 0.6	CEM II B-M 0.5	CEM III B 0.6	CEM III B 0.5	CEM I 0.6	CEM I 0.5
12 days								
21 days								
38 days								
61 days								
82 days								
101 days								
145 days								
160 days								

### 5.2.2. Concrete natural carbonation

The first test of carbonation penetration for the natural CO<sub>2</sub> concentration was performed after 10 months from production and 7 months from exposure at 65% RH. The results are reported in Table 3. The deepest carbonation was found for CEM II/B-LL and CEM III/B with 0.6 w/b, where it reached approx. 5 mm. For the same w/b, CEM II/B-M seemed more resistant to carbonation (depth approx. 3-4 mm), while CEM I was the most resistant (depth approx. 2-3 mm). The 0.5 w/b mixes clearly showed less carbonation than the 0.6 w/b mixes.

Table 3 Thymolphthalein test to assess the accelerated carbonation depth for the different concrete mixes.

CEM II/B-LL 0.6	CEM II/B-LL 0.5	CEM II/B-M 0.6	CEM II/B-M 0.5
			
CEM III/B 0.6	CEM III/B 0.5	CEM I 0.6	CEM I 0.5
			

### 5.2.3. Corrosion rate of steel rebars in concrete

Table 4 summarizes the corrosion rate measurements of phase 2, performed on the concrete specimens. The data in the table is the result of monitoring the corrosion rate over time, the results reported include an average and standard deviation of 3 measurements per sample type and exposure condition. The values in the table are the corrosion rates at steady state, that is when the corrosion rate has stabilized and is constant.

Table 4 Summary of corrosion rates of Phase 2. What is reported is an average over at least 3 measurements per mix and exposure condition, with the standard deviation. Note that 1  $\mu\text{A}/\text{cm}^2$  corresponds to approx. 12  $\mu\text{m}/\text{y}$ .

		Corrosion rate ( $\mu\text{A}/\text{cm}^2$ )							
Binder		CEM I		CEM II/B-LL		CEM II/B-M		CEM III/B	
w/b		0.5	0.6	0.5	0.6	0.5	0.6	0.5	0.6
Moisture state	95% RH	0.09 $\pm 0.03$	0.17 $\pm 0.02$	0.27 $\pm 0.12$	0.45 $\pm 0.12$	0.15 $\pm 0.05$	0.20 $\pm 0.07$	0.21 $\pm 0.05$	0.36 $\pm 0.05$
	WET	0.37 $\pm 0.09$	0.59 $\pm 0.27$	0.87 $\pm 0.39$	1.93 $\pm 0.74$	0.40 $\pm 0.16$	1.01 $\pm 0.34$	0.58 $\pm 0.18$	2.03 $\pm 0.70$

### 5.2.4. Influence of Binder type and w/b

Figure 8a shows the corrosion rates measured in the concrete specimens, divided by binder type, for the two moisture states. It appears that steel embedded in CEM II/B-LL and CEM III/B corrode slightly faster than in CEM I and CEM II/B-M. However, the ratio between binders remains within a factor 2 and 3. The same applies for the w/b, Figure 7b shows the data grouped to highlight only the w/b effect, which seems to be comparable to the one of the binder type, in the range that was studied in our work (w/b 0.5 and 0.6).

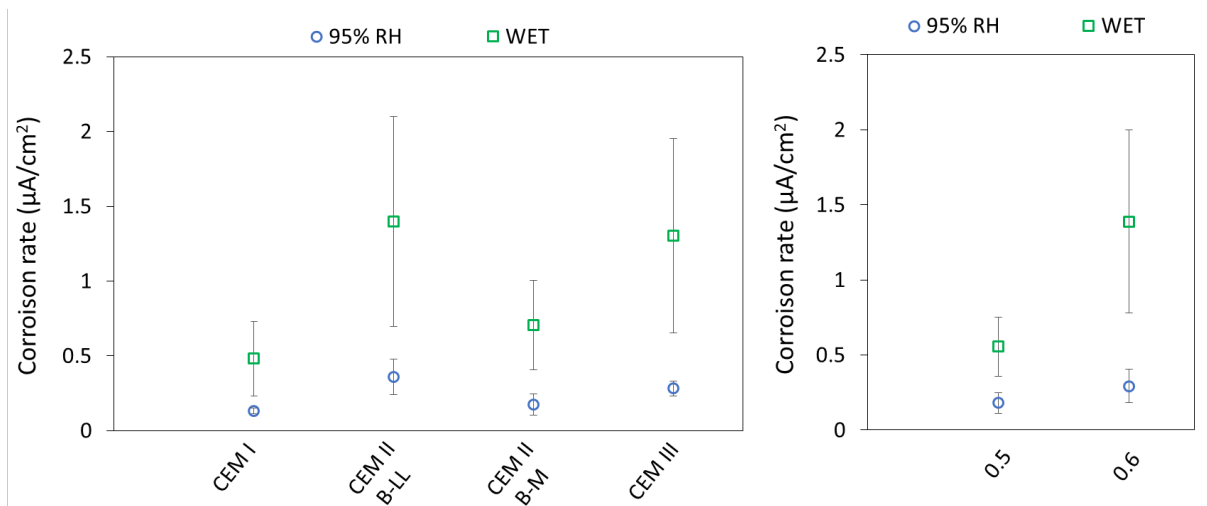


Figure 8 Corrosion rates in concrete specimens, grouped by binder type (a) and w/b (b). The markers are the average of all corrosion rates measured for the specific binder (a) or w/b (b); the whiskers are the standard deviation. Note that 1  $\mu\text{A}/\text{cm}^2$  corresponds to approx. 12  $\mu\text{m}/\text{y}$ .

### 5.2.5. Influence of humidity exposure condition

The humidity of exposure impacts greatly the corrosion rate. Figure 9 reports the limits that are usually considered for a rough estimation of the corrosion risk. Only in WET conditions is the corrosion rate just above the threshold of medium risk, while for 95% RH the values are in the low risk range. In WET conditions we measured a corrosion rate about 5 times higher than at 95% RH.

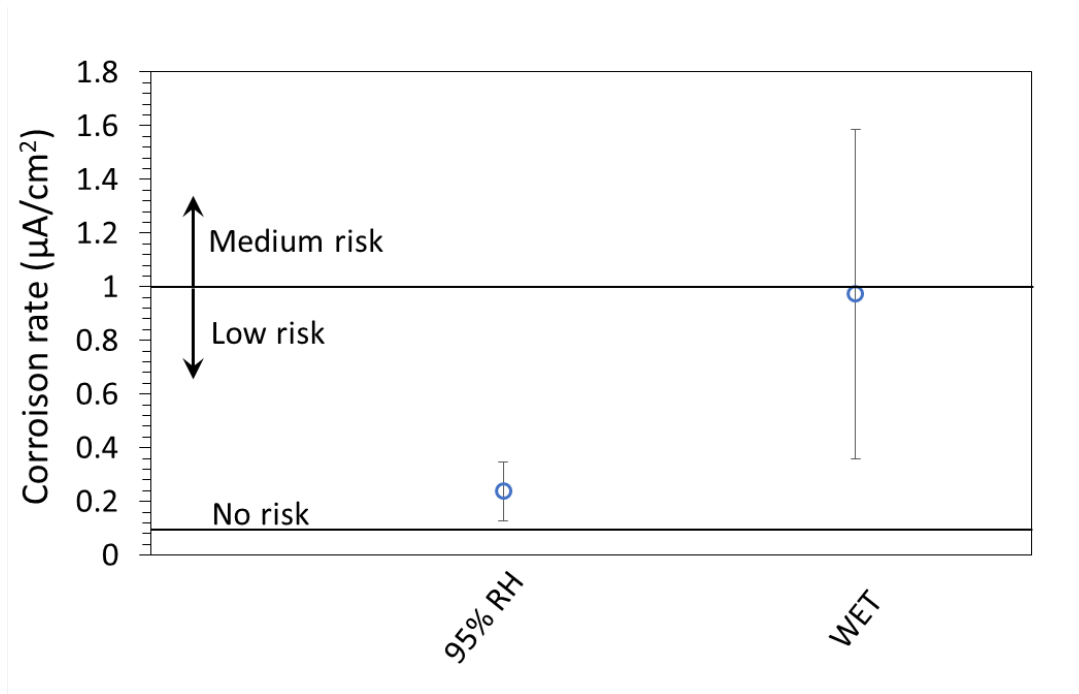


Figure 9 Corrosion rates in concrete specimens, grouped per humidity exposure condition. The markers are the average of all corrosion rates measured at the specific humidity condition; the whiskers are the standard deviation. The thresholds (medium, low, no risk) are based on L. Bertolini et al. "Corrosion of Steel in Concrete", WILEY-VCH, 2003). Note that 1  $\mu\text{A}/\text{cm}^2$  corresponds to approx. 12  $\mu\text{m}/\text{y}$ .

### 5.2.6. Concrete porosity

The porosity of the different carbonated mixes was calculated by considering it as the available space for water ingress. Therefore, the porosity that is reported in Table 5 is considered an estimate for the capillary porosity of the concrete samples used in this study.

Looking at the results, CEM II/B-LL and CEM III/B mixes show a similar porosity, while a decrease can be noticed for CEM II/B-M and a further decrease for CEM I. As expected, a lower w/b leads to lower porosity. The range that could be calculated with the method here used goes from a low capillary porosity of 10.6% (CEM I 0.5) to a high porosity of 16.3% (CEM II/B-LL 0.6). It should be noted that the different systems were tested at the same age (they were all cured at 95% RH for 3 months before being carbonated), and thus, different degrees of hydration are expected.



*Table 5 Experimentally determined porosity. The porosity is an estimate of the capillary porosity of the carbonated concretes.*

Mix	Porosity (-)
CEM II/B-LL 0.6	0.163
CEM II/B-LL 0.5	0.138
CEM III/B 0.6	0.159
CEM III/B 0.5	0.137
CEM II/B-M 0.6	0.150
CEM II/B-M 0.5	0.121
CEM I 0.6	0.131
CEM I 0.5	0.111

## 6. Discussion

### 6.1. Comparison between corrosion rates of Phase 1 and Phase 2

An essential point of this study was to use the measurements of corrosion rate in concrete samples (Phase 2) in order to confirm the measurements performed on mortar samples (Phase 1), where the rebars were substituted with steel wires and the cementitious matrix differed (mortar vs. concrete). Figure 9 compares the results from the two phases, for the same exposure conditions. The corrosion rate is here plotted as an average among all mixes. For 95% RH the corrosion rate agreed very well for the mortar and concrete samples, while for WET conditions the average corrosion rate was about 30% lower for concrete samples with respect to the mortar samples. An explanation of this lower corrosion rate in the concrete samples compared to the mortar samples in WET conditions might be that it was difficult for the water to penetrate through a concrete cover of centimetres, while it was easier to penetrate through the 3 mm cover of the smaller mortar samples. In the experiments, it was noticed that it was necessary to extend the wetting period for the concrete samples in Phase 2 up to 7 days in order to achieve a sufficiently stable corrosion rate. Extending the waiting time even further may have reduced the difference between mortar and concrete even further. In fact, looking at the results in more detail, the difference in corrosion rate between mortar (Phase 1) and concrete (Phase 2) was highest for the samples with the lowest porosity ( $w/b=0.5$  and CEM I).

Nevertheless, it should be noted that, considering the standard deviations (Figure 10), the difference of 30% in corrosion rate is hardly statistically significant. Moreover, considering the effect of the moisture condition on the corrosion rate, the difference found between mortar and concrete as well as between steel wires and rebars, is considered small or negligible. It can thus be concluded that the results obtained with the small mortar samples are reliable and representative of corrosion rates in concrete.

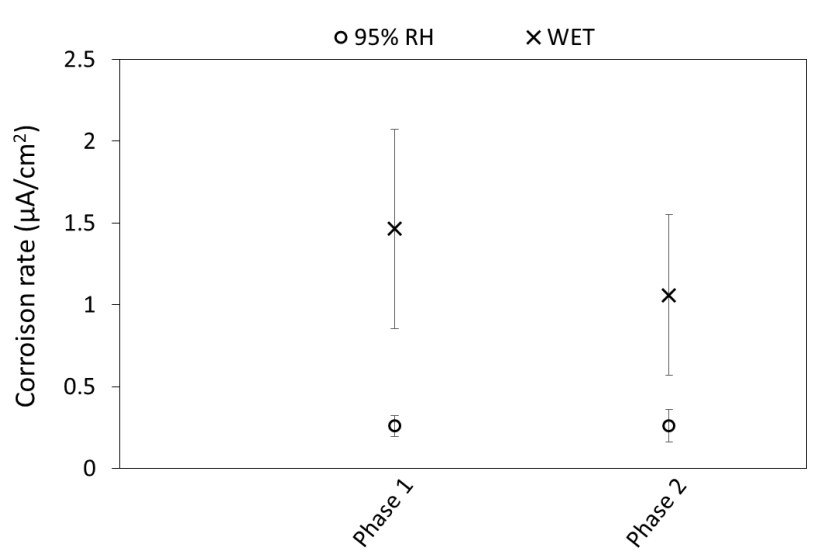


Figure 10 Comparison of corrosion rate results obtained from Phase 1 (mortar samples) and Phase 2 (concrete samples) for the humidity exposure conditions 95% RH and WET. The marker is the average of all corrosion rates measured in each phase, at the specific humidity condition; the whiskers are the standard deviations. Note that 1  $\mu A/cm^2$  corresponds to approx. 12  $\mu m/y$ .

## 6.2. Relationship between corrosion rate and capillary porosity in Phase 2

As already found in previous work, there might be a close causality link between concrete porosity and steel corrosion rate in a carbonated environment [8]. This is due mainly to the fact that the amount of steel surface area that gets in contact with water is directly dependent on the porosity of the cementitious matrix surrounding the steel. Therefore, a correlation is expected when the two parameters are plotted together. Figure 11 shows that such relationship does exist for the experimentation of Phase 2 in this work. There is a general trend of corrosion rate increase with higher porosity concrete. This correlation may be fitted with a linear or an exponential function, with little difference in the result for the materials studied here.

It should be noted that CEM I (in carbonated state) showed the lowest porosity, while the CEM II and CEM III concretes (in carbonated state) exhibited higher porosities (Table 5).

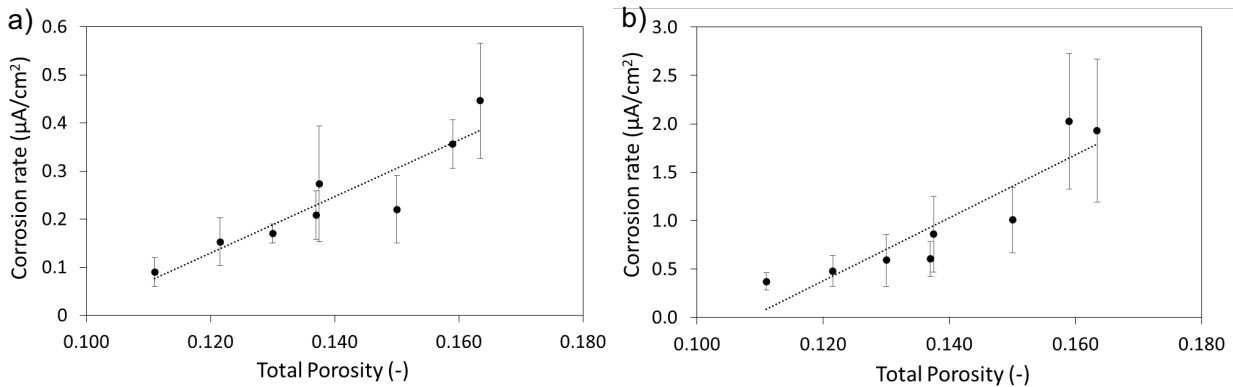


Figure 11 Relationship between corrosion rate and porosity for the reinforced concrete specimens used in Phase 2. a) Corrosion rate for exposure to 95% RH. b) Corrosion rate for WET conditions. Note that  $1 \mu\text{A}/\text{cm}^2$  corresponds to approx.  $12 \mu\text{m}/\text{y}$ .

## 6.3. Influence of the aggregates on carbonation-induced corrosion rate

The experiments carried out in Phase 1 showed that there was no statistically significant variation of corrosion rate due to a variation of the aggregate size distribution. Now, the agreement between the corrosion rates measured in Phase 1 (mortar) and 2 (concrete) confirms this observation. This may be explained by the fact that the corrosion rate is most likely controlled by the porous system that is present at the steel-concrete interface, which is mainly dependent on the cement paste, as the wall effect leads to the formation of a cement paste layer in contact with the steel. Accordingly, the influence of aggregate particles further away is limited.

## 6.4. Factors influencing the corrosion rate

Several environmental and material factors were investigated. Here, the results are summarized in order to draw conclusions on the magnitude of their effect (Figure 12). The influencing factors are below ranked according to their importance.

- Humidity of exposure: the moisture state it is surely the most pronounced influencing parameter. In this study the effect was of a factor 10 for a relatively small range of humidity (95% RH to WET conditions). In literature it is common to find a factor of more than 100 when the range of humidity 50% RH to WET is considered.
- Temperature: the second environmental parameter has a smaller effect on the corrosion rate, in the studied temperature range (5-40 °C) the corrosion rate varies of a factor < 3. The effect of temperature could be more pronounced if we expanded the range.
- Binder type: the effect of binder type is less pronounced than the one of the environmental parameters, by changing the binder, the corrosion rate is affected by a factor < 3. The binders seem divided into two groups, with CEM I and CEM II/B-M showing relatively low corrosion rates and CEM II/B-LL and CEM III/B leading to higher ones.
- w/b: in the small range studied (w/b = 0.5-0.6), the w/b ratio is the least relevant parameter, with the corrosion rate being affected by a factor of approx. 2. Of course, in case of a wider range of w/b, the effect may increase.

The environmental parameters seem to be more relevant than the material parameters. According to the numbers just summarized, the corrosion rate over the year could change over a factor 300 or higher, depending on the humidity condition and the temperature alone. On the materials side, the concrete mix design can affect the steel corrosion rate by a factor up to 10, if we merge the contributions of binder type and w/b ratio, which can include a wider range than what has been studied in this work.

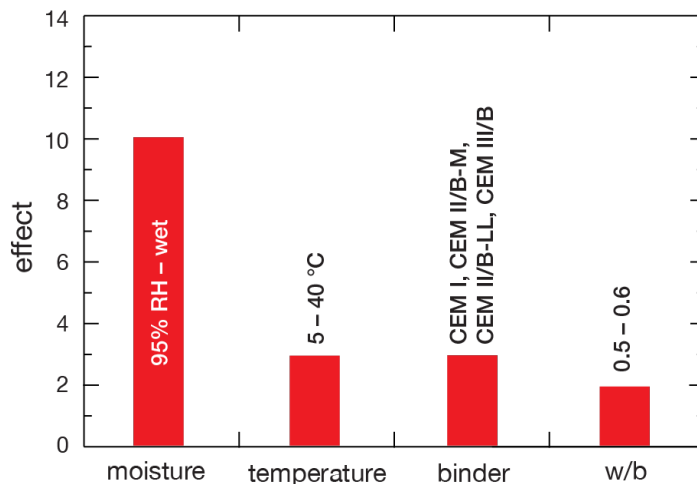


Figure 12 Visual representation of influencing factors for the corrosion rate in carbonated concrete: moisture, temperature, binder type, and w/b ratio. Studied ranges indicated.

## 7. Conclusions

From the results obtained in this project, it is possible to draw the following conclusions on the corrosion behaviour of steel in carbonated concrete:

- The environmental conditions affect the corrosion rate strongly, and to a much larger extent than the mix design.
- The most important environmental parameter is the moisture state, with a factor 10 on the instantaneous corrosion rate even for a relatively small range of humidity (95% RH to WET conditions). The temperature, in the studied range, had a moderate impact, with a change of a factor 3 in the temperature range between 5 and 40 °C.
- For exposure conditions drier than 95% RH, the instantaneous corrosion rates are around or less than 2 µm/y. Corrosion rates of concern under most practical conditions are thus only expected for very moist conditions (RH > 95%).
- The investigated binder types as well as w/b ratios had an influence on the corrosion rate, however, at least one order of magnitude below the influence of the moisture state. Nevertheless, the corrosion rate was found to be affected by binder type and/or w/b ratio by a factor of up to 3. The binders can be divided into two groups, with CEM I and CEM II/B-M showing relatively low corrosion rates and CEM II/B-LL and CEM III/B leading to higher ones.
- Varying the aggregate size in the mortar samples had a negligible effect on the corrosion rates of the embedded steel. Similarly, comparing the small laboratory scale samples (steel wires in mortar) to larger scale samples (rebar in concrete) led to comparable results in terms of instantaneous corrosion rates upon exposure to a certain moisture state.
- Since there exists a relationship between the corrosion rate of the steel and the capillary porosity of the concrete, the capillary porosity of carbonated mortar/concrete may be used as a “durability indicator” in an attempt to roughly quantify the effect of different mixes (binder type, mix proportions) on the expected corrosion rate.
- This study suggests that corrosion rates determined in laboratory scale studies (mortar, steel wires as opposed to concrete and reinforcing steel bars) are applicable to concrete structures. Or in other words: The material side is not decisive, but the exposure conditions – that can differ considerably between lab and site conditions – are.

These conclusions contribute to considering the corrosion propagation stage in service life modeling.



## 8. Outlook

### 8.1. On the important role of moisture in the concrete cover

In this work, values of corrosion rate were quantified for carbon steel embedded in carbonated concrete with different selected binders, different w/b ratios, different moisture and temperature exposure conditions. It appears that a relevant risk of carbonation-induced corrosion damage only arises in case of high water presence at the steel surface. The next question to tackle now is how these conditions are generally achieved (and for how long) in structures, in particular in wet/dry exposure conditions, such as XC4 according to the European standards. This ultimately comes down to quantifying the moisture state in the concrete (at the rebars depth) and over time. The concrete cover, supposed to protect the steel from the low pH of a carbonated environment, might also be perceived as a barrier against water penetration. In this frame, it would be important to understand:

- The relationship between the time of wetness of the concrete surface and the depth of the water front inside the concrete.
- Can we design a system in such a way that the moisture condition at the rebar level (in the carbonated concrete) can be controlled and kept below a critical limit (such as 95% RH)?
- How to integrate exposure conditions, such as local micro-climates, adequately into design approaches?

### 8.2. Amount of corrosion leading to damage (cracking, spalling)

Another important question left for further study is how much accumulated corrosion attack (e.g. in terms of  $\mu\text{m}$ ) finally leads to cracking of the concrete cover. In order to understand the propagation stage of corrosion in the service life of a structure, and therefore being able to predict how long it would take to develop carbonation-induced damage, it is necessary to understand the amount of corrosion that finally creates enough pressure to damage the concrete surrounding the rebars.

## 9. References

- [1] Bertolini, Luca, Bernhard Elsener, Pietro Pedferri, Elena Redaelli, and Rob Polder, *Corrosion of steel in concrete: prevention, diagnosis, repair*, John Wiley & Sons, 2013.
- [2] M. Stefanoni, U. M. Angst and B. Elsener, «Corrosion rate of carbon steel in carbonated concrete – A critical review» *Cement and Concrete Research*, Bd. 103, pp. 35-48, 2018.
- [3] EN 206+1 Concrete – Part 1: Specification, performance, production and conformity, European Committee for Standardization, 2006.
- [4] Olivier, Jos GJ, Greet Janssens-Maenhout, Marilena Muntean, and J. A. H. W. Peters, *Trends in global CO2 emissions: 2015 Report*, The Hague: PBL Netherlands Environmental Assessment Agency, 2015.
- [5] Oggioni, G., R. Riccardi, and R. Toninelli, «Eco-efficiency of the world cement industry: a data envelopment analysis» *Energy Policy*, Bd. 39, Nr. 5, pp. 2842-2854, 2015.
- [6] Leemann, Andreas, Peter Nygaard, Josef Kaufmann, and Roman Loser, «Relation between carbonation resistance, mix design and exposure of mortar and concrete» *Cement & Concrete Composites*, Bd. 62, pp. 33-43, 2015.
- [7] M. Stefanoni, U. M. Angst and B. Elsener, «Electrochemistry and capillary condensation theory reveal the mechanism of corrosion in dense porous media» *Scientific Reports*, Bd. 8, Nr. 1, 2018.
- [8] M. Stefanoni, U. M. Angst and B. Elsener, «Kinetics of electrochemical dissolution of metals in porous media» *Nature Materials*, Bd. 18, Nr. 9, pp. 942-947, 9 2019.
- [9] T. Jaśniok and M. Jaśniok, «Influence of rapid changes of moisture content in concrete and temperature on corrosion rate of reinforcing steel» in *Procedia Engineering*, 2015.
- [10] J. M. Deus, B. Díaz, L. Freire and X. R. Nóvoa, «The electrochemical behaviour of steel rebars in concrete: An Electrochemical Impedance Spectroscopy study of the effect of temperature,» *Electrochimica Acta*, Bd. 131, pp. 106-115, 10 6 2014.
- [11] M. Pour-Ghaz, O. Burkan Isgor and P. Ghods, «The effect of temperature on the corrosion of steel in concrete. Part 2: Model verification and parametric study» *Corrosion Science*, Bd. 51, Nr. 2, pp. 426-433, 1 2 2009.
- [12] M. Stefanoni, U. M. Angst and B. Elsener, «Innovative sample design for corrosion rate measurement in carbonated concrete» in *11th annual International Concrete Sustainability Conference (2016 ICSC)*, Washington DC, 2016.
- [13] M. Stefanoni, U. M. Angst and B. Elsener, «A New Setup for Rapid Durability Screening of New Blended Cements» in *Concrete Innovation Conference (CIC2017)*, Trosno, 2017.